Impact of Dispersion Fluctuations on 40-Gb/s Dispersion-Managed Lightwave Systems

Ekaterina Poutrina, *Student Member, IEEE, Student Member, OSA,* and Govind P. Agrawal, *Fellow, IEEE, Fellow, OSA*

***Abstract*—We study numerically the impact of random dispersion fluctuations on the performance of 40-Gb/s dispersion-managed lightwave systems designed using either the chirped return-to-zero or the soliton format and employing backward-pumped distributed Raman amplification. We consider two-section dispersion maps with $\beta_2 = \pm 4$ and ± 8 ps^2/km and show that the Q parameter decreases rapidly in both cases as the nonlinear effects become stronger. The impact of dispersion fluctuations can be reduced by lowering the average input power, but the system length is then limited by amplifier noise.**

***Index Terms*—Dispersion fluctuations, dispersion management, distributed Raman amplification, nonlinear optics, optical fiber communication, optical solitons.**

I. Introduction

THE performance of modern dispersion-managed (DM) lightwave systems depends on a large number of factors, the two most important being the noise added by optical amplifiers and the nonlinear effects taking place inside the fiber link [1]. It has become apparent in recent years that the dispersion of an optical fiber, which is designed to have a fixed value, can vary over a considerable range because of unavoidable variations in the core diameter along the fiber length [2]–[6]. Even though such axial variations are static, they can impact the system performance because of the nonlinear nature of the pulse propagation problem. A second source of dispersion fluctuations is related to environmental changes. For example, if temperature fluctuates at a given location, the local dispersion would also change in a random fashion. Such dynamic fluctuations can also degrade the system performance. Although dispersion fluctuations rarely impact a 10-Gb/s system, their role on the system performance must be considered for 40-Gb/s lightwave systems for which dispersion tolerance is relatively tight.

In this paper, we present the results of extensive numerical simulations performed to identify the impact of dispersion fluctuations on the performance of 40-Gb/s DM lightwave systems. Although dispersion fluctuations have been considered in some recent papers [7]–[10], the emphasis was mostly on the broadening of a single pulse transmitted through the fiber link. In contrast, we model a realistic lightwave system in which a data-coded pulse train consisting of 0 and 1 bits is transmitted through a periodically amplified DM fiber link. The system performance is quantified by the well-known Q parameter that is related to the bit-error rate in a simple way. Our emphasis is on identifying how the nonlinear effects are affected by dispersion fluctuations and how the local value of average dispersion affects the interplay among the nonlinear effects and dispersion fluctuations.

The paper is organized as follows. We discuss in Section II the numerical approach and focus on the nonsoliton systems based on the chirped return-to-zero (CRZ) format. In Section III, we consider DM soliton systems. We first address the questions of the optimization of input parameters for a given dispersion map and then investigate the influence of dispersion fluctuations on the system performance. The main conclusions of the paper are summarized in Section IV.

II. CRZ Systems

Propagation of optical pulses in single-mode fibers is described by the nonlinear Schrödinger equation [11]

$$\frac{\partial u}{\partial z} = -i\frac{\widetilde{\beta}_2}{2}\frac{\partial^2 u}{\partial t^2} + i\gamma_0 |u|^2 u + \frac{1}{2}(g - \alpha_s)u + f_n(z,t) \quad (1)$$

where $g(z)$ and α_s(z) account, respectively, for the local gain and signal loss inside the fiber, $\gamma_0(z)$ is the nonlinear coefficient, $\widetilde{\beta}_2(z)$ is the second-order dispersion parameter, and $f_n(z,t)$ represents the contribution of noise along the fiber length. This equation is written for the case of distributed Raman amplification. We use this technique of amplification for our simulations because it provides a better signal-to-noise ratio (SNR) compared with lumped fiber amplifiers and is rapidly being adopted in practice.

We solve (1) numerically using the split-step Fourier method and model dispersion fluctuations as

$$\widetilde{\beta}_2(z) = \beta_2(z) + \delta\beta_2(z) \quad (2)$$

where $\beta_2(z)$ is the average value of local dispersion and $\delta\beta_2(z)$ is a small random variable assumed to have a Gaussian distribution with zero mean. In numerical simulations, we change $\delta\beta_2$ every step size (0.3 km) along the fiber length using a Gaussian random variable with zero mean and with standard deviation of up to $0.2\beta_2(z)$. We use 15 different realizations of stochastic Gaussian process representing 15 different fiber links. To account for the amplified spontaneous emission (ASE) noise for each of the 15 links, the Q parameter (defined later) is evaluated by averaging over an ensemble of 1280 pulses, realized by repeated propagation of a 64-bit pseudorandom bit sequence with 20 different ASE noise realizations. Since time-dependent dispersion fluctuations happen on quite a long time scale (> 1 μs),

Manuscript received September 24, 2002. This work was supported in part by the National Science Foundation under Grant ECS-9903580 and Grant DMS-0073923.

The authors are with the Institute of Optics, University of Rochester, Rochester, NY 14627 USA (e-mail: poutrina@optics.rochester.edu).

Digital Object Identifier 10.1109/JLT.2003.810101

there are no dynamic fluctuations during a single run for a bit stream of 128 bits or less. Assuming static and dynamic dispersion fluctuations to be independent events, the impact of both types of fluctuations can be treated by considering the results of propagation of the same bit stream over multiple fiber links with different realizations of dispersion fluctuations.

We start by considering a perfectly linear 40-Gb/s system. For numerical simulations, we use two dispersion maps. Each map consists of two fiber sections of nearly equal length (5 km) with opposite signs of the dispersion parameter (but the same absolute value). For map 1, $\beta_2 = \pm 4$ ps^2/km, while for map 2, $\beta_2 = \pm 8$ ps^2/km. In both cases, the average dispersion $\beta_2^{\rm av}$ is -0.01 ps^2/km, and $L_{\rm A} = 8L_{\rm m} = 80$ km, where $L_{\rm A}$ and $L_{\rm m}$ are the amplification and the map periods, respectively. We adopt the dense DM technique ($L_{\rm m} << L_{\rm A}$) because its use improves the performance of 40-Gb/s systems especially when DM solitons are used [12]. Nonlinearity is set to zero ($\gamma_0 = 0$) temporarily and losses are included such that $\alpha_{\rm s} = 0.2$ dB/km in each fiber section. We employ the technique of Raman distributed amplification with backward pumping for compensating fiber losses. The gain profile $g(z)$ is obtained by solving the appropriate equations for the Raman amplification process [11]. The pump power is chosen such that $\int_0^{L_{\rm A}} g(z)dz = \alpha_s L_A$. We use 6-ps input pulses with the input chirp $C_0 = 0.3$. We also use optical filters with 400-GHz bandwidth separated by $L_{\rm A}$.

We calculate the Q parameter in two ways. The first measure Q_1 uses the detector current filtered with a Butterworth filter of 35 GHz ($\Delta {\rm f} = 0.875$ B) at the receiver. More specifically, Q_1 is calculated using [1]

$$Q_1 = \frac{I_1 - I_0}{\sigma_1 + \sigma_0} \tag{3}$$

where I_1 and I_0 are the average values for 1 and 0 bits at the center of the bit slot, and σ_1 and σ_0 are the corresponding standard deviations. In this approach, I_1 and I_0 correspond to the peak power of the optical pulse (assuming that the timing jitter introduced by Raman amplification is negligible). In the second approach, we calculate the optical Q parameter by using the pulse energy obtained by integrating over the entire bit slot and define Q as

$$Q_2 = \frac{E_1 - E_0}{\sigma_1 + \sigma_0} \tag{4}$$

where E_1 and E_0 are the average energies for 1 and 0 bits and σ_1 and σ_0 are the corresponding standard deviations.

For the 15 fiber links, we find the Q parameter (averaged over 1280 pulses for each fiber link) as a function of propagation distance for several values of the standard deviation of local dispersion. As an example, Fig. 1 shows the Q_1 parameter for all 15 fiber links for the map with $\beta_2 = \pm 8$ ps^2/km with 5% of dispersion fluctuations, which corresponds to the standard deviation $\sigma_{\rm D}$ of local dispersion of 0.4 ps^2/km for this map. The input peak power of each pulse is $P_0 = 2$ mW, which corresponds to an average power of 0.42 mW for the pseudorandom bit sequence. The insert shows the Q_1 parameter in the absence of fluctuations. We see that, in the linear case, the Q parameter does not change much in the presence of fluctuations for all 15

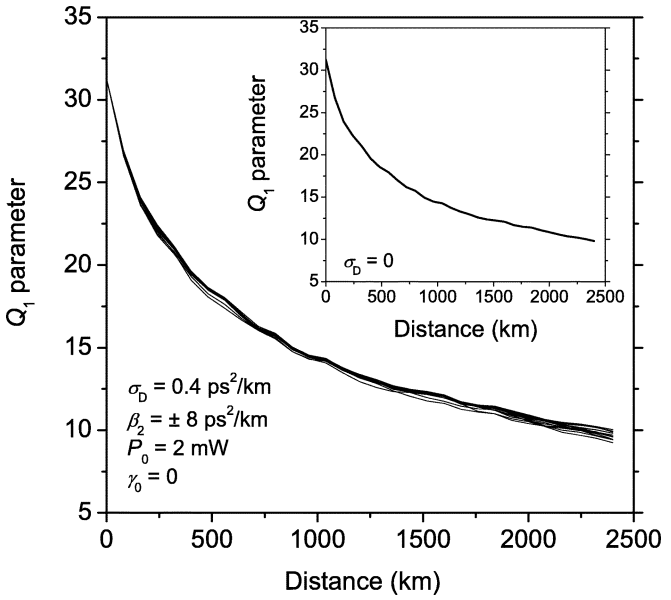

Fig. 1. Influence of dispersion fluctuations in a linear 40-Gb/s CRZ DM system with $\beta_2 = \pm 8$ ps^2/km. The Q_1 parameter is shown as a function of distance for 15 fiber links with 5% dispersion fluctuations (standard deviation $\sigma_{\rm D} = 0.4$ ps^2/km). The insert shows Q_1 in the absence of fluctuations.

fiber links used. The reason for the small difference in Q along the distance for 15 fiber links comes from additional accumulated dispersion $d_r = \int_0^L \delta\beta_2(z)dz$ that varies randomly for different fibers. This additional contribution broadens the pulse even more during signal propagation [7],[8]. The value and the sign of this additional broadening depend on $d_{\rm r}$ [8]. This random broadening leads to a change in the Q value. For the 15 fiber links used, $d_{\rm r}$ at 2400 km ranged from -12.6 ps^2 to 22.8 ps^2 when 5% of dispersion fluctuations were introduced, while the deterministic value of accumulated dispersion at this distance is -24 ps^2.

We consider now the worst case Q parameter at 2400 km. Fig. 2 shows the dependence of the worst case Q for the two maps on the standard deviation of dispersion fluctuations. The levels of fluctuations used correspond to the standard deviation $\sigma_{\rm D}$ ranging from 0 to 20% of the local dispersion value. For each value of standard deviation, the same 15 sequences of random numbers, scaled accordingly, were used, and the fiber link with the worst value of Q at 2400 km was then considered.

As seen in Fig. 2, the Q parameter decreases in all cases, even in a purely linear system, as the standard deviation of dispersion fluctuations increases. Although this decrease is relatively slow, eventually Q becomes small enough that the system will be limited by dispersion fluctuations. The decrease of the Q parameter with increased β_2 fluctuations even for a linear system is due to the larger values of $d_{\rm r}$ for larger amounts of fluctuations. The results indicate that, for a given fiber link, Q can be improved by post-compensating or periodically compensating the accumulated random dispersion.

We note from Fig. 2 that Q_1 is up to 1.1 dB larger than Q_2. The reason is related to the fact that Q_1 samples the pulse power at the bit center while Q_2 measures the pulse energy spread over the entire bit. As a result, the Q_1 parameter is much more sensitive to timing jitter than Q_2. This result suggests that the use of

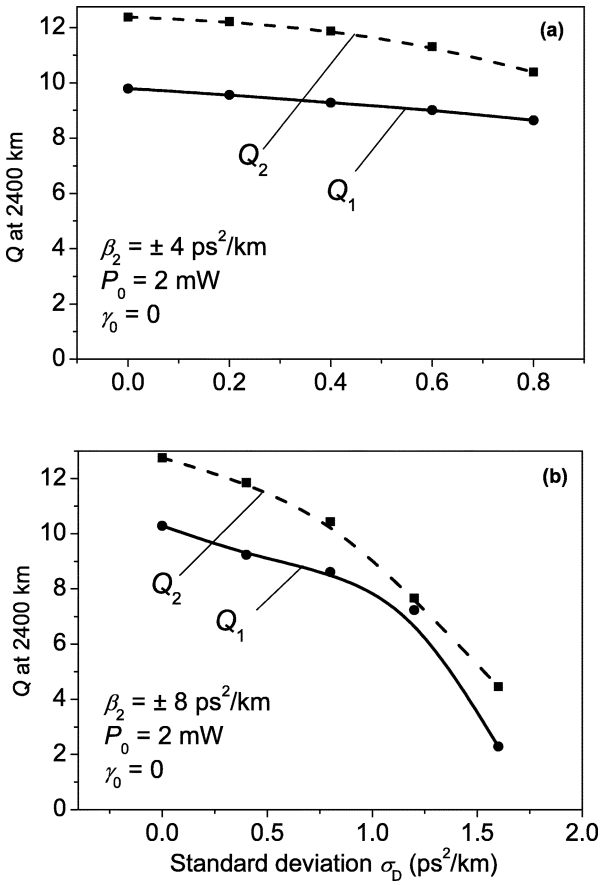

Fig. 2. Worst case Q parameter at 2400 km for two linear 40-Gb/s CRZ DM systems. Dispersion map is such that (a) $\beta_2 = \pm 4$ ps^2/km and (b) $\beta_2 = \pm 8$ ps^2/km. Solid and dashed lines show Q_1 and Q_2 calculated using peak powers and pulse energies, respectively.

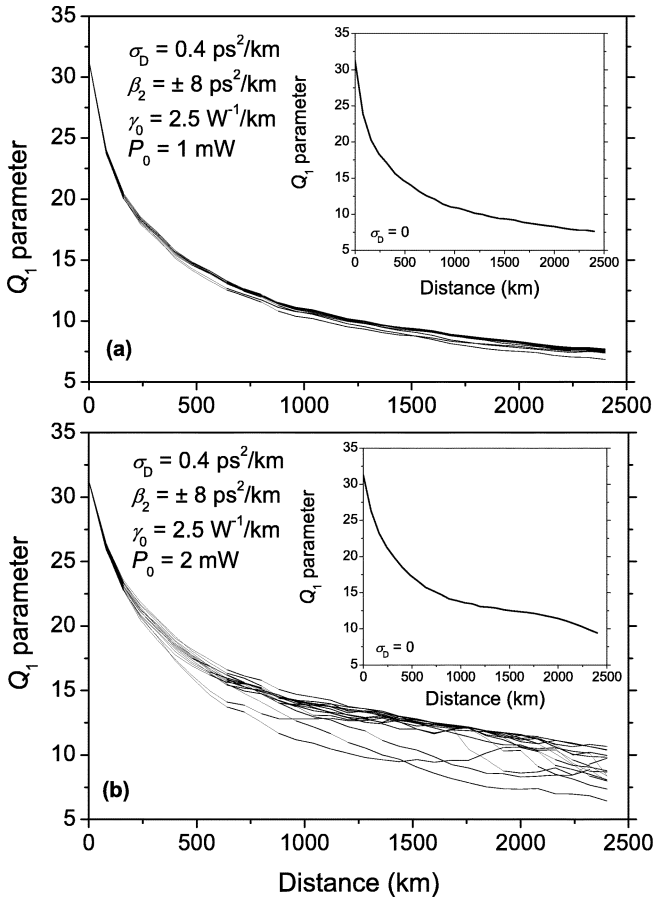

Fig. 3. Influence of dispersion fluctuations in the presence of nonlinearity for the same 40-Gb/s CRZ system shown in Fig. 1. The inserts show Q_1 in the absence of fluctuations. The input peak powers are (a) 1 mW and (b) 2 mW.

a receiver that integrates the signal over the bit slot rather than makes a measurement at one point would improve the system performance. Since most receivers currently sample the signal at the bit center, we use the Q_1 parameter for system characterization in this paper.

The results shown in Fig. 2 were obtained by turning off the nonlinear term in (1) by setting $\gamma_0 = 0$. However, the nonlinearity is inherent in any real system. In the presence of nonlinearity, the pulse propagation is affected by the interplay between the local dispersion and nonlinearity (rather than being dependent only on the total accumulated dispersion). We consider next how the impact of dispersion fluctuations is changed when the nonlinear effects are taken into account by choosing $\gamma_0 = 2.5$ W^{-1}/km in all fiber sections.

Fig. 3 shows the Q_1 parameter as a function of distance for the 15 fiber links for the DM system with $\beta_2 = \pm 8$ ps^2/km using $P_0 = 1$ and 2 mW. For both peak power levels, the standard deviation of local dispersion is 5% (0.4 ps^2/km). The inserts show Q_1 in the absence of fluctuations. We see that, as nonlinear effects become stronger, the impact of dispersion fluctuations on system performance becomes much more noticeable. While the decrease in Q_1 at 2400 km is at most 0.46 dB for 1-mW peak power, it becomes 1.8 dB at 2 mW.

For any peak power, larger fluctuations lead to more degradation. As an example, the worst case Q_1 parameter at a peak power of 1.5 mW is shown in Fig. 4 for several levels of $\sigma_{\rm D}$. We see that fluctuations with $\sigma_{\rm D} = 1.6$ ps^2/km can lead to about 6.5-dB degradation of the Q parameter. We note also that, for all fiber links considered, the worst case Q at 2400 km for CRZ systems is usually obtained in the fiber that has the largest random accumulated dispersion $d_{\rm r}$ at 2400 km.

The results of Figs. 3 and 4 are summarized in Fig. 5, which shows the worst case Q_1 at 2400 km for several values of input peak power as a function of $\sigma_{\rm D}$. Comparing with Fig. 2, we see that in all cases the Q parameter degrades much faster with increasing dispersion fluctuations than in a linear system. The rate of degradation increases when the nonlinear effects are intensified using larger input powers.

For any CRZ system, an optimum input power exists that provides the best system performance for a certain propagation distance [13]. For input powers smaller than the optimum, the CRZ system becomes limited by noise added by amplifiers, while for larger input powers it is limited by the increased nonlinear effects. An example of such a behavior at a distance of 2400 km for the 40-Gb/s system designed with $\beta_2 = \pm 8$ ps^2/km is shown in Fig. 6, where we plot Q_1 as a function of input power. The optimum peak power in the absence of dispersion fluctuations is about 2 mW. Even 5% dispersion fluctuations (standard deviation 0.4 ps^2/km) reduce the optimum peak power to near 1.3 mW while lowering the value of Q by about

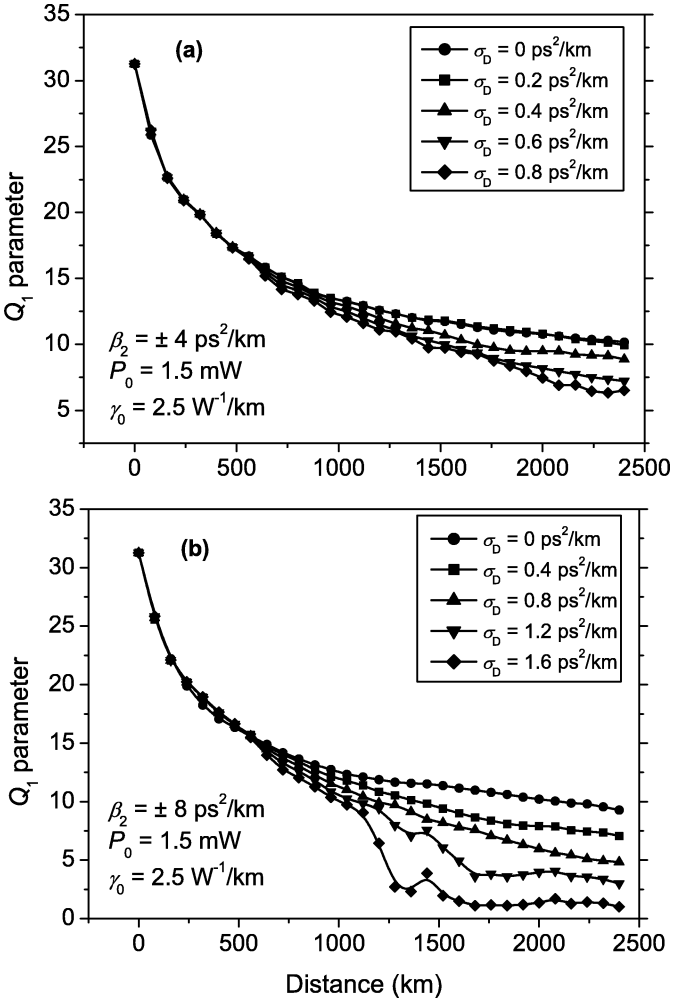

Fig. 4. Dependence of the worst case Q_1 parameter on transmission distance for several values of $\sigma_{\rm D}$. Dispersion maps are such that (a) $\beta_2 = \pm 4$ ps^2/km and (b) $\beta_2 = \pm 8$ ps^2/km.

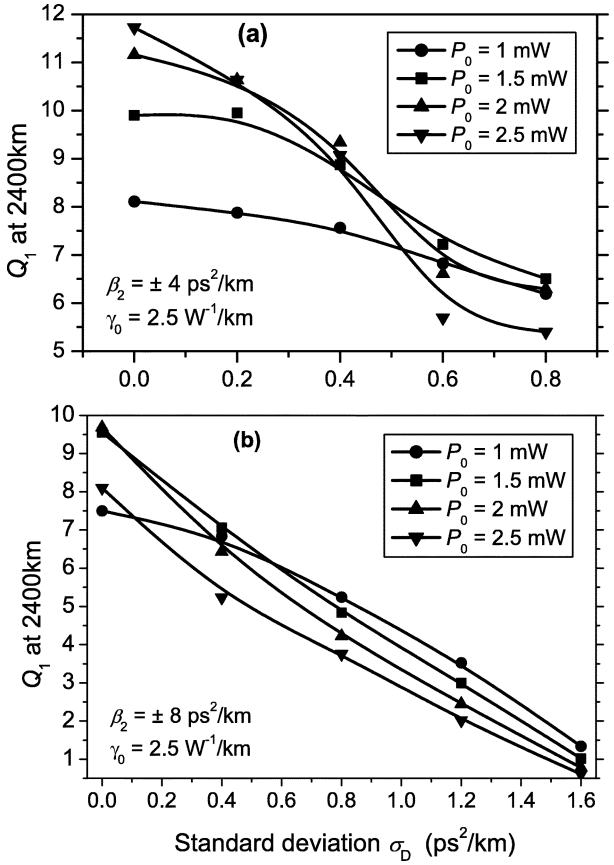

Fig. 5. Effect of dispersion fluctuations on Q_1 at several peak power levels for the same two systems shown in Fig. 2, except that the nonlinear effects are turned on by setting $\gamma_0 = 2.5$ W^{-1}/km.

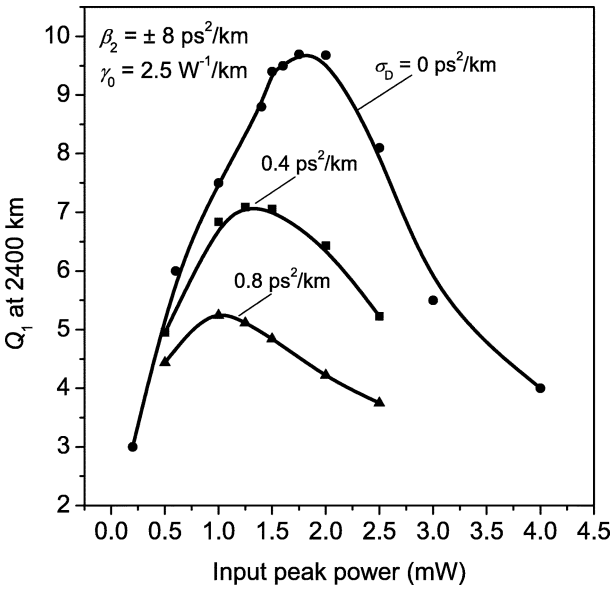

Fig. 6. Dependence of the worst case Q_1 parameter on the input peak power for the same 40-Gb/s system shown in Fig. 5(b) for several levels of dispersion fluctuations.

26%. Larger values of fluctuations make the situation worse. To increase the system tolerance to dispersion fluctuations it may be better, according to Figs. 5 and 6, to use input peak powers slightly less than the optimum value predicted in the absence of fluctuations.

III. DM Soliton Systems

A natural question is how the impact of dispersion fluctuations on system performance is affected when DM solitons are used as bits. In this section, we answer this question. Since DM soliton systems require a balance between the dispersive and nonlinear effects, the presence of dispersion fluctuations might break this balance and degrade the system performance even more. We study how much the rate of degradation increases when the input power and, hence, the nonlinear effects in DM soliton system become larger.

The new feature of DM solitons is that the system is designed such that the pulse in each bit slot recovers its width, chirp, and energy after each amplification period. Thus, all pulse parameters vary periodically during the propagation with a period equal to $L_{\rm A}$. The periodicity can be ensured only if the input pulse parameters have specific values for a given dispersion map. As shown in [12], the input width of a chirped pulse T_0 and the

input energy E_0 can be found using the following relations:

$$T_0 = T_{\rm map}\sqrt{\frac{1+C_0^2}{|C_0|}} \tag{5}$$

$$E_0 = k\,2\sqrt{2\pi}\,\frac{\beta_{21}\varepsilon_1(l_1)+\beta_{22}\varepsilon_2(l_2)}{\left(\frac{\gamma_{01}}{\sqrt{c_1}}\right)\ln r_1+\left(\frac{\gamma_{02}}{\sqrt{c_2}}\right)\ln r_2} \tag{6}$$

where $T_{\rm map}$ is a parameter with dimensions of time involving the four map parameters

$$T_{\rm map} \equiv \left|\frac{\beta_{21}\beta_{22}l_1l_2}{\beta_{21}l_1-\beta_{22}l_2}\right|^{\frac{1}{2}} \tag{7}$$

while ε_1, r_i, and $c_i (i = 1 \text{ or } 2)$ are given by

$$\varepsilon_i(z) \equiv \frac{1}{2}\frac{c_i - a_ib_i}{\sqrt{c_i^3 b_i}}\left[\tan^{-1}\left(\sqrt{\frac{c_i}{b_i}}\,(l_i)\right) - \tan^{-1}\left(\sqrt{\frac{c_i}{b_i}}\,(l_i-2z)\right)\right] \tag{8a}$$

$$r_i = \frac{T_0 - l_i\sqrt{c_i}}{T_0 + l_i\sqrt{c_i}}, \quad a_i \equiv \frac{C_0^2}{l_i^2},$$

$$b_i \equiv \pm\frac{1}{2}\beta_{2i}C_0l_i + T_0^2, \quad c_i \equiv \mp\frac{\beta_{2i}C_0}{2l_i}. \tag{8b}$$

We note that T_0 is the width of the chirped pulse at the beginning of the map period, while the minimum pulsewidth at the chirp-free point inside the map is given by $T_{\rm m} = T_{\rm map}/|C_0|$ [12]. In (6), constant k depends on the kind of amplification scheme used and, in the region $|C_0| \lesssim 1.3$, is equal to $k = \{(1/L_A)\int_0^{L_A}\exp[\int_0^z(g(z')-\alpha_s(z'))dz']dz\}^{-1}$, $g(z)$ being the local gain and $\alpha_s(z)$ being signal loss in the system.

Equations (5) and (6) provide the values of input pulsewidth and energy as functions of input chirp. According to (5), the input pulsewidth T_0 has a minimum value $T_0^{\rm min} = \sqrt{2}\,T_{\rm map}$ when the input chirp is $|C_0| = 1$. In this case, the minimum pulsewidth $T_{\rm m}$ at the chirp-free point is equal to the map parameter $T_{\rm map}$, and the pulse is stretched by a factor of $\sqrt{2}$ during propagation. As discussed in [12], in the absence of noise but accounting for intrachannel pulse interactions, the best pulse propagation occurs near this region $|C_0| \approx 1$, $E_0 \approx E_{\rm c}$, where $E_{\rm c}$ is the value of input energy corresponding to $|C_0| = 1$. An example of the input parameters for chirp values ranging from 0.03 to 3 is shown in Fig. 7 for the same two maps used in the CRZ case. Solid lines are obtained by solving the variational equations [1] numerically, while circles represent the values obtained by using (5) and (6). The inserts show the input energy and input width as functions of input chirp. We see that, as predicted by (5), the input pulsewidth has a minimum at $E_{\rm c}$ corresponding to $|C_0| = 1$. In this section, we consider several input parameters sets, with the energies ranging from $E_{\rm c}$ to $\approx 5E_{\rm c}$, where the nonlinear effects become quite strong. The sets of input parameters used are shown with arrows in Fig. 7. For comparison purposes, we employ the same two dispersion maps used earlier for CRZ systems. We note from (7) that reducing the length of fiber segments decreases the $T_{\rm map}$ parameter, which helps to increase the possible bit rate of a DM soliton system [12]. For that reason, dense dispersion management is used in this paper. The map parameter is $T_{\rm map} \approx 3.17$ ps and $T_{\rm map} \approx 4.47$ ps for systems with $\beta_2 = \pm 4$ and ± 8 ps^2/km, respectively.

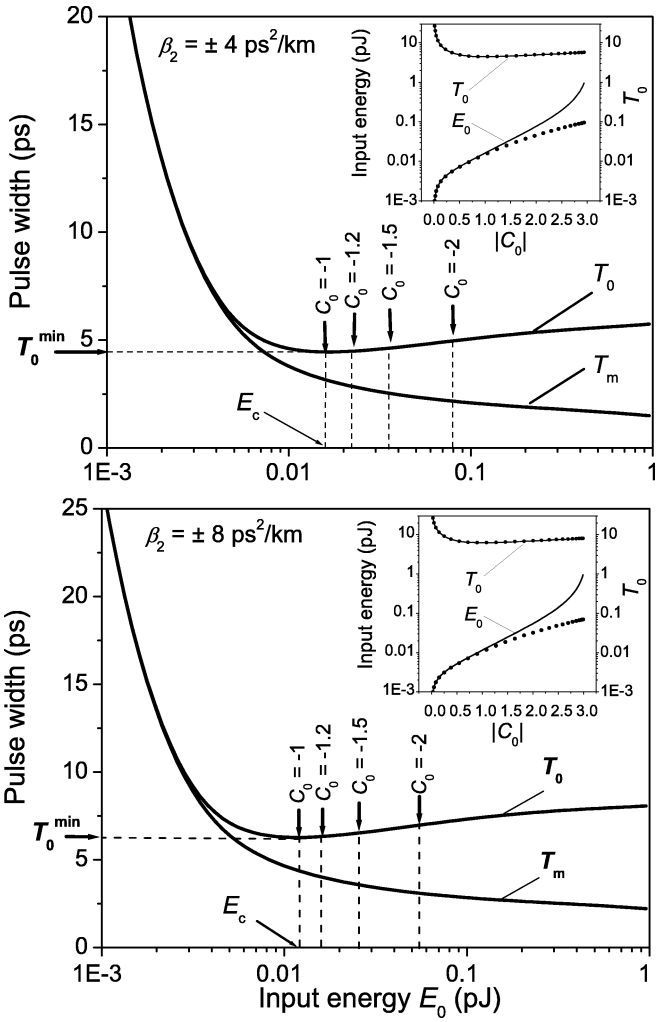

Fig. 7. Input pulsewidth T_0 and corresponding minimum pulsewidth $T_{\rm m}$ at the chirp-free point for a DM soliton system plotted as functions of the input pulse energy. The insert shows the dependence of input energy and pulsewidth on input chirp. The arrows indicate the input pulse parameters used in Figs. 8 and 9 simulations. Solid lines are numerical values; circles are analytical results.

We consider the same 15 fiber links with random dispersion fluctuations as in the CRZ case. Fig. 8 shows the Q_1 parameter as a function of distance for the map $\beta_2 = \pm 8$ ps^2/km for input parameters sets corresponding to $C_0 = -1.2$ and -2. The level of fluctuations is 5% ($\sigma_{\rm D} = 0.4$ ps^2/km) for both sets of input parameters. The inserts show Q_1 in the absence of fluctuations. Since the input energy is increased for $C_0 = -2$, the nonlinear effects are much stronger in this case and the Q parameter is affected much more by dispersion fluctuations than in system with $C_0 = -1.2$. We have chosen to label the graphs with the input chirp C_0 because, as described above, the optimization of this parameter will apply to almost any dispersion map while the optimum value of pulse energy is map dependent.

The dependence of the worst case Q_1 parameter on the standard deviation of β_2 at a distance of 2400 km is shown on Fig. 9 for several input parameters sets. The $\sigma_{\rm D}$ values are in the range

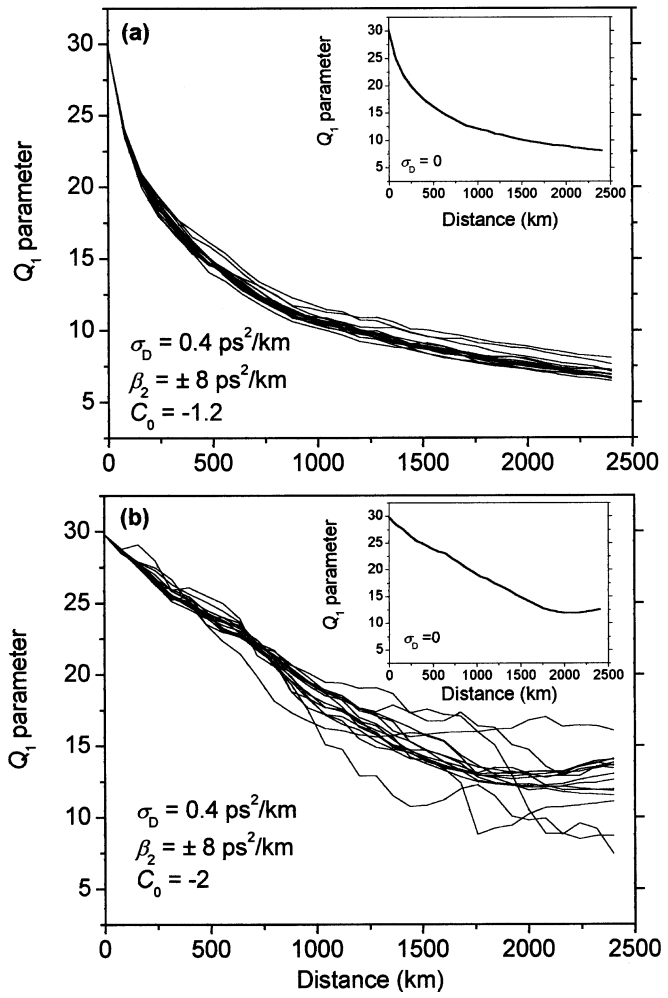

Fig. 8. Effect of dispersion fluctuations on Q_1 parameter for a DM soliton system for the same map used in Fig. 3. The input parameters are obtained from Fig. 7 for (a) $C_0 = -1.2$ and (b) $C_0 = -2.0$.

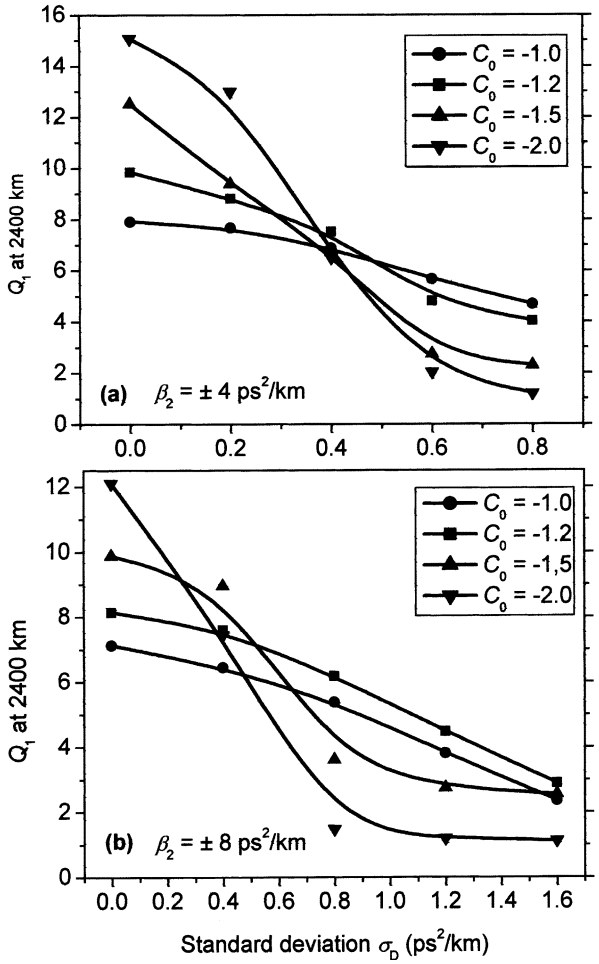

Fig. 9. Effect of dispersion fluctuations on Q_1 parameter in DM soliton systems for the same two dispersion maps used in Fig. 5.

from 0 to 20% of the local dispersion for each map. Similarly to the CRZ case, the use of higher energy pulses (and higher average power at the input end) decreases the system tolerance to dispersion fluctuations. This behavior is the same for both maps. In the absence of both noise and dispersion fluctuations ($< \delta\beta_2^2 >= 0$), the optimum value of the Q parameter is obtained for input chirp values near 1.1 [12]. In the presence of noise but without dispersion fluctuations, Q increases for larger values of C_0 because the use of higher energy pulses improves the SNR while the nonlinear effects are balanced by the use of DM solitons. However, dispersion fluctuations change this behavior because they perturb the balance between the dispersive and nonlinear effects. For example, in the presence of 10% dispersion fluctuations, it is better to reduce the pulse energy by lowering the chirp in the neighborhood of $C_0 = 1.2$. We conclude that while accounting for both noise and dispersion fluctuations, the optimum input parameters should remain in the region around $C_0 \approx 1.2$. Comparing DM solitons with the CRZ case, we note that Q_1 decreases with increasing β_2 fluctuations in nearly the same manner, suggesting that the impact of dispersion fluctuations does not depend on the use of solitons as long as the RZ format is employed.

IV. Concluding Remarks

In this paper, we have investigated numerically the influence of second-order dispersion fluctuations on the performance of 40-Gb/s systems designed with distributed Raman amplification. We have considered both the CRZ and DM soliton formats and used the Q parameter for judging the system performance. We have shown that dispersion fluctuations can lead to performance degradation even in a linear system when the change in the total accumulated dispersion, introduced by fluctuations, is not completely compensated. The presence of nonlinearity aggravates the extent of system degradation induced by dispersion fluctuations for both CRZ and DM soliton systems. We have shown that this degradation increases fast when the nonlinear effects in the system are made stronger by using higher energy pulses. The system tolerance to dispersion fluctuations can be improved by employing a receiver that integrates the signal over some portion of the bit slot, rather than making a measurement at the center of the bit slot. We discussed the impact of dispersion fluctuations on the optimum input parameters and showed that, for CRZ systems, one should use the input peak powers slightly smaller than the optimum values predicted in the absence of fluctuations. For DM soliton systems, accounting for both noise and the presence of dispersion fluctuations, the optimum input pulsewidth and pulse energy should be calculated

from (5) and (6) by choosing $C_0 \approx 1.2$. For such values of C_0, the map strength is about 1.65, and the effects of intrapulse interaction are also minimized [12]. Although we have focused on single-channel system in this paper, the preceding discussion should apply even for wavelength division multiplexed (WDM) systems.

In our simulations, dispersion values were changed after every step, in effect making the correlation length of dispersion fluctuations equal to the step size (0.3 km). The correlation length l_c in actual fibers may vary over a considerable range and is not often known precisely. Our results can be used for other values of l_c by noting that the product ${\sigma_D}^2 l_c$ determines the extent of pulse broadening for long link lengths [8], where ${\sigma_D}^2$ is the variance of dispersion fluctuations. Thus, one should scale σ_D with l_c such that ${\sigma_D}^2 l_c$ remains constant.

Finally, we note that the fluctuations of the second-order dispersion β_2 result from the static or dynamic fluctuations in the frequency-dependent refractive index. This implies that fluctuations are present in all orders of dispersion. When the refractive index fluctuations are dynamic, including the first-order dispersion fluctuations results in the presence of one more fluctuating term in the nonlinear Schrödinger equation that depends on fluctuations in the group velocity and can lead to a new source of timing jitter. However, if dynamic fluctuations happen on a sufficiently long time scale, the effect of fluctuations in the group velocity may be compensated electronically.

ACKNOWLEDGMENT

The authors would like to thank D. Chowdhury, S. Kumar, and Q. Lin for helpful discussions.

REFERENCES

[1] G. P. Agrawal, *Fiber-Optic Communication Systems*, 3rd ed. New York: Wiley, 2002.

[2] H. Onaka, K. Otsuka, H. Miyata, and T. Chikama, "Measuring the longitudinal distribution of four-wave mixing efficiency in dispersion-shifted fibers," *IEEE Photon. Technol. Lett.*, vol. 6, pp. 1454–1457, Dec. 1994.

[3] K. Ishiba, K. Tadayoshi, and T. Mikio, "Soliton system evaluations using fibers with dispersion and loss fluctuations," *Electron. Commun. Jpn.*, pt. 2, vol. 79, pp. 780–786, Apr. 1996.

[4] L. F. Mollenauer, P. V. Mamyshev, and M. J. Neubelt, "Method for facile and accurate measurement of optical fiber dispersion maps," *Opt. Lett.*, vol. 21, pp. 1724–1726, Nov. 1996.

[5] K. Nakajima, M. Ohashi, and M. Tateda, "Chromatic dispersion distribution measurement along single-mode optical fiber," *J. Lightwave Technol.*, vol. 15, pp. 1095–1101, July 1997.

[6] J. Gripp and L. F. Mollenauer, "Enhanced range for OTDR-like dispersion map measurements," *Opt. Lett.*, vol. 23, pp. 1603–1605, Oct. 1998.

[7] F. Kh. Abdulaev and B. B. Baizakov, "Disintegration of a soliton in a dispersion-managed optical communication line with random parameters," *Opt. Lett.*, vol. 25, pp. 93–95, Jan. 2000.

[8] Q. Lin and G. P. Agrawal, "Pulse broadening induced by dispersion fluctuations in optical fibers," *Opt. Commun.*, vol. 206, pp. 313–317, Apr. 2002.

[9] F. Kh. Abdulaev, J. C. Bronski, and G. Papanicolaou, "Soliton perturbations and the random Kepler problem," *Phys. D*, vol. 135, pp. 369–386, Jan. 2000.

[10] Y. Takushima, T. Douke, W. Xiaomin, and K. Kikuchi, "Dispersion tolerance and transmission distance of a 40-Gb/s dispersion management soliton transmission system," *J. Lightwave Technol.*, vol. 20, pp. 360–367, Mar. 2002.

[11] G. P. Agrawal, *Nonlinear Fiber Optics*, 3rd ed. New York: Academic, 2002, ch. 2.

[12] E. Poutrina and G. P. Agrawal, "Design rules for dispersion-managed soliton systems," *Opt. Commun.*, vol. 206, pp. 193–200, June 2002.

[13] L. J. Richardson, V. K. Mezentsev, and S. K. Turitsyn, "Limitations of 40 Gb/s based dispersion managed WDM transmission: Solitons versus quasilinear propagation regime," presented at the *Optical Fiber Communications Conf.*, Mar. 2001, paper MF5.

Ekaterina Poutrina (S'03) received the M.S. degree from Moscow State University, Moscow, Russia, in 1991. She is currently working toward the Ph.D. degree with the Institute of Optics, University of Rochester, Rochester, NY.

From 1991 to 1998, she conducted research at Moscow State University and taught at the Moscow State Technical University. Her research interests include nonlinear fiber optics, optical communication system design, as well as propagation and interaction of electromagnetic waves in nonuniform structures.

Ms. Poutrina is a Student Member of the Optical Society of America (OSA).

Govind P. Agrawal (F'96) received the B.S. degree from the University of Lucknow, Lucknow, India, in 1969 and the M.S. and Ph.D. degrees from the Indian Institute of Technology, New Delhi, in 1971 and 1974, respectively.

After holding positions at the Ecole Polytechnique, France, the City University of New York, New York, and AT&T Bell Laboratories, Murray Hill, NJ, he joined the faculty of the Institute of Optics at the University of Rochester, Rochester, NY, in 1989, where he is a Professor of Optics. His research interests focus on quantum electronics, nonlinear optics, and laser physics. In particular, he has contributed significantly to the fields of semiconductor lasers, nonlinear fiber optics, and optical communications. He is an author or coauthor of more than 300 research papers, several book chapters and review articles, and five books entitled *Semiconductor Lasers* (Norwell, MA: Kluwer, 2nd ed., 1993), *Fiber-Optic Communication Systems* (New York: Wiley, 3rd ed., 2002), *Nonlinear Fiber Optics* (New York: Academic, 3rd ed., 2001), *Applications of Nonlinear Fiber Optics* (New York: Academic, 2001), and *Optical Solitons: From Fibers to Photonic Crystals* (New York: Academic, 2003). He has also edited two books *Contemporary Nonlinear Optics* (New York: Academic, 1992) and *Semiconductor Lasers: Past, Present and Future* (New York: AIP, 1995).

Dr. Agrawal is a Fellow of the Optical Society of America (OSA). He has participated many times in organizing the technical conferences sponsored by the IEEE and OSA. He was the Program Co-Chair and the General Co-Chair of the Quantum Electronics and Laser Science Conference in 1999 and 2001, respectively. He also chaired a program subcommittee for the conference on Nonlinear Guided Waves and their Applications in 2001.